Selective replication of oncolytic virus M1 results in a bystander killing effect that is potentiated by Smac mimetics

Jing Cai[a,1], Yuan Lin[a,b,1], Haipeng Zhang[a], Jiankai Liang[a], Yaqian Tan[a], Webster K. Cavenee[c,2], and Guangmei Yan[a,2]

[a]Department of Pharmacology, Zhongshan School of Medicine, Sun Yat-sen University, Guangzhou 510080, China; [b]Department of Medical Statistics and Epidemiology, School of Public Health, Sun Yat-sen University, Guangzhou 510080, China; and [c]Ludwig Institute for Cancer Research, University of California, San Diego, CA 92093-0660

Contributed by Webster K. Cavenee, May 24, 2017 (sent for review January 18, 2017; reviewed by Raymond Bergan and Samuel D. Rabkin)

Oncolytic virotherapy is a treatment modality that uses native or genetically modified viruses that selectively replicate in and kill tumor cells. Viruses represent a type of pathogen-associated molecular pattern and thereby induce the up-regulation of dozens of cytokines via activating the host innate immune system. Second mitochondria-derived activator of caspases (Smac) mimetic compounds (SMCs), which antagonize the function of inhibitor of apoptosis proteins (IAPs) and induce apoptosis, sensitize tumor cells to multiple cytokines. Therefore, we sought to determine whether SMCs sensitize tumor cells to cytokines induced by the oncolytic M1 virus, thus enhancing a bystander killing effect. Here, we report that SMCs potentiate the oncolytic effect of M1 in vitro, in vivo, and ex vivo. This strengthened oncolytic efficacy resulted from the enhanced bystander killing effect caused by the M1 virus via cytokine induction. Through a microarray analysis and subsequent validation using recombinant cytokines, we identified IL-8, IL-1A, and TRAIL as the key cytokines in the bystander killing effect. Furthermore, SMCs increased the replication of M1, and the accumulation of virus protein induced irreversible endoplasmic reticulum stress- and c-Jun N-terminal kinase–mediated apoptosis. Nevertheless, the combined treatment with M1 and SMCs had little effect on normal and human primary cells. Because SMCs selectively and significantly enhance the bystander killing effect and the replication of oncolytic virus M1 specifically in cancer cells, this combined treatment may represent a promising therapeutic strategy.

oncolytic virus | SMAC mimetics | bystander killing effect

Oncolytic viruses are replicating microorganisms that specifically replicate in and kill tumor cells without causing harm to normal cells (1). Some viruses have a natural preference for tumor cells, whereas others can be engineered to replicate in and lyse tumor cells (2). The cancer tropism and safety of oncolytic viruses make them promising anticancer biological agents, and there are many ongoing or completed clinical trials using oncolytic viruses belonging to at least 10 different virus families (2). Encouraging results were obtained in 2015, when the US Food and Drug Administration approved talimogene laherparepvec, which is derived from HSV and was genetically engineered to express granulocyte/macrophage colony stimulating factor for melanoma patients (3, 4), making it the first oncolytic virus approved to treat patients.

We have previously identified M1, a strain of Getah-like alphavirus isolated from culicine mosquitoes in the Hainan province of China, as an oncolytic virus that induces endoplasmic reticulum (ER) stress-mediated apoptosis in zinc-finger antiviral protein (ZAP)-deficient cancer cells (5, 6). Recently, M1 was reported to be nonpathogenic in nonhuman primates after multiple rounds of repeated i.v. injections (7). Although oncolytic viruses selectively kill tumor cells, the outcome of infection with them varies a lot due to the complex interactions between the virus and the host defense system (8). This fact has led to efforts aimed at increasing the effects of oncolytic viruses by genetically modifying or combining them with chemical sensitizers (1, 2, 9–14). This fact has also prompted us to test whether combining M1 with various chemical compounds enhances the oncolytic effect in refractory tumor cells in which M1 inhibits less than 25% of cell viability (15). For example, we recently reported that the activation of cyclic adenosine monophosphate (cAMP) and exchange protein directly activated by cAMP1 (Epac1) signaling pathways enhances the oncolytic effect of M1 (15, 16), which supports our hypothesis.

Viral infection causes the release of viral pathogen-associated molecular patterns and cellular danger-associated molecular patterns, which activate the host innate immune system to secrete cytokines, such as TNF-α, TRAIL, IFN-γ, IL-12, as well as dozens of other cytokines and chemokines (17–19). Current perspective supports that the immune response to oncolytic virus appears to be a critical component of the antitumor immune effect (8, 11).

Inhibitors of apoptosis protein (IAPs) comprise a family of antiapoptotic proteins that promote prosurvival signaling pathways and prevent the activation of caspases (20). The most studied and classical IAPs are caspase-IAP1 (c-IAP1), c-IAP2, and X-linked IAP (XIAP). Second mitochondria-derived activator of caspases (Smac), a natural IAP inhibitor in the mitochondria, can

Significance

Although oncolytic therapy is showing great potential in clinical trials, not all patients benefit from it. Combining oncolytic viruses with anticancer chemicals could provide a better chance to increase the response rate. Here, we report that the combination of an alphavirus (M1) that we identified previously and second mitochondria-derived activator of caspases (Smac) mimetic compounds (SMCs) shows substantial oncolytic effect in vitro, in vivo, and ex vivo (samples from patients' tumor tissues). The combined effect is mediated by a bystander killing effect and increased replication of M1. Our work provides an example for potentiating the response rate in refractory samples by synergizing oncolytic virus with other anticancer chemicals. We predict that this treatment strategy will be a promising tool to combat cancer in the future.

Author contributions: J.C., Y.L., and G.Y. designed research; H.Z., J.L., and Y.T. performed research; J.C., Y.L., W.K.C., and G.Y. analyzed data; and J.C., Y.L., W.K.C., and G.Y. wrote the paper.

Reviewers: R.B., Oregon Health Sciences University; and S.D.R., Massachusetts General Hospital and Harvard Medical School.

The authors declare no conflict of interest.

Data deposition: The data reported in this paper have been deposited in the Gene Expression Omnibus (GEO) database, https://www.ncbi.nlm.nih.gov/geo (accession no. GSE92918).

[1]J.C. and Y.L. contributed equally to this work.

[2]To whom correspondence may be addressed. Email: wcavenee@ucsd.edu or ygm@mail.sysu.edu.cn.

This article contains supporting information online at www.pnas.org/lookup/suppl/doi:10.1073/pnas.1701002114/-/DCSupplemental.

activate caspase and promote apoptosis by binding to several IAPs via its amino-terminal acid residues (21), leading to the elimination of the inhibitory effect of IAPs. Due to its proapoptotic role, Smac mimetic compounds (SMCs) were developed as anticancer agents, and some SMCs have been evaluated in early- to midstage clinical trials (20). Moreover, various researchers have reported that by inhibiting the function of IAPs, SMCs sensitize tumor cells to the bystander killing effect induced by cytokines, such as TNF-α (22–24), TRAIL (22, 25, 26), and IL-1β (27). We therefore reasoned that SMCs may also potentiate the bystander killing effect mediated by virus-induced cytokines.

To determine whether SMCs potentiate the oncolytic effect of M1 in refractory tumor cells and to explore whether SMCs sensitize tumor cells to the bystander killing effect induced by M1, we combined SMCs [LCL161 (28) and birinapant (29)] with M1 in refractory tumor cells. Here, we report that by specifically targeting c-IAP1 and c-IAP2, SMCs sensitize tumor cells to cytokines induced by M1 and increase its replication. We also verified the potentiated oncolytic effect in vivo and ex vivo. Taken together, combination of SMCs and M1 shows great potential against tumors and provides a promising therapeutic strategy for patients who have cancer in the future.

Results

SMCs Potentiate M1-Induced Apoptosis in Tumor but Not Normal Cells. To explore whether SMCs potentiate the oncolytic effect of M1 in refractory tumor cells, we chose four tumor cell lines [two hepatocellular carcinoma cell lines (Huh-7 and PLC) and two colorectal carcinoma cell lines (HCT 116 and SW620); blue columns in Fig. 1*A*] in which M1 has only minor inhibitory effects on cell viability (Fig. 1*A*). LCL161 exerts a cytotoxic effect on these cells when the concentration is higher than 5 μM (Fig. S1*A*), which is considered as the maximal noneffective dose and was chosen to examine the combined effect. On combination, the SMCs LCL161 and birinapant significantly increased M1-induced cell death in each of the four cell lines in both the LCL161 dose-dependent and M1 dose-dependent manners (Fig. S1 *B* and *C*). Moreover, in another two M1-sensitive cell lines (LoVo and Hep3B) and two M1-resistant cell lines (Hep-G2 and SK-HEP-1), SMC LCL161 failed to potentiate the oncolytic effect of M1 (Fig. S1*D*), indicating that the combination strategy applies to tumors that are midsensitive to M1 virus. To understand whether the combination is synergistic, we calculated the IC_{50} value for each treatment with nonlinear regression (vertical dotted lines in Fig. S1 *A* and *E*), as well as the combination index (CI) (30) under IC_{50}. The CIs in HCT 116 and Huh-7 cells were 0.21 and 0.16, respectively (Fig. 1*B*) (CI < 1, CI = 1, and CI > 1 indicate synergism, additivity, and antagonism, respectively), indicating that the combination of SMCs and M1 is synergistic. The dead tumor cells in the combined treatment group showed severe karyopyknosis with Hoechst 33342 staining (red arrows in Fig. 1*C* and Fig. S1*F*), indicating apoptosis of the cells. As expected, M1 alone could slightly induce the activities of caspase-3/7, caspase-8, and caspase-9, but the activities of caspase-3/7, caspase-8, and caspase-9 were dramatically elevated after treatment with the combination of M1 and LCL161 (Fig. 1*D* and Fig. S1*G*).

To explore the safety of the combined strategy, the normal colorectal cell line NCM460, normal hepatic cell line L-02, and three types of human normal primary cells (human hepatocytes, human aortic endothelial cells, and human corneal epithelial cells) were treated with SMC LCL161 or birinapant plus M1. Neither M1 alone nor the combined treatment significantly reduced cell viability (Fig. S1 *H* and *I*). These results suggest that SMCs potentiate caspase-3/7–, caspase-8–, and caspase-9–dependent apoptosis induced by M1 in multiple tumor cells but not in normal cells.

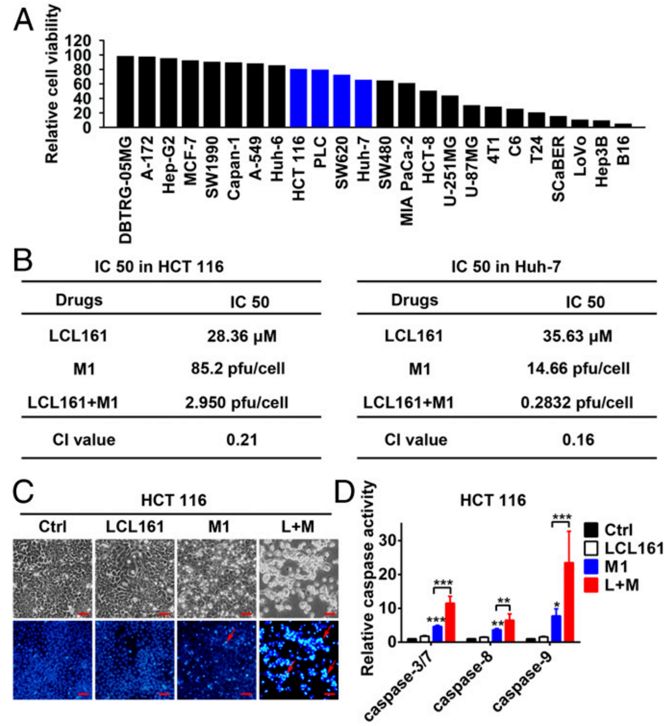

Fig. 1. SMCs enhance M1-induced apoptosis in tumor cells. (*A*) Relative cell viability in 24 tumor cell lines treated with M1 [multiplicity of infection (MOI) = 1 plaque-forming unit per cell (pfu/cell), 48 h]. (*B*) IC_{50} and CI values in HCT 116 and Huh-7 cells. IC_{50} values are indicated in Fig. S1 *A* and *D* by vertical dotted lines, and the calculation formula for the CI is detailed in *SI Materials and Methods*. (*C*) Phase-contrast and Hoechst 33342 staining (5 μg/mL for 10 min) of HCT 116 cells treated with M1 (MOI = 1 pfu/cell) with or without 5 μM LCL161 for 72 h. (Scale bars: 50 μm.) (*D*) Relative activities of caspase-3/7, caspase-8, and caspase-9 were detected in HCT 116 cells treated as in *C*. Error bars represent mean ± SD obtained from three independent experiments. Ctrl, control; L+M, LCL161 + M1. *$P < 0.05$; **$P < 0.01$; ***$P < 0.001$.

SMCs Potentiate the Bystander Killing Effect Triggered by M1. Interestingly, in the combined treatment group, some of the dead HCT 116 and Huh-7 cells showed severe karyopyknosis with Hoechst 33342 staining but were not infected with iRFP-tagged M1 (yellow arrows in Fig. 2*A* and Fig. S2*A*), indicating cell death in the neighboring uninfected cells. Further, we detected the percentage of apoptotic cells among the infected and uninfected cells on combined treatment using flow cytometry. Most of the apoptotic cells were uninfected with M1 virus (black columns in Fig. 2*B* and Fig. S2*B*). These results suggest that the combination of SMCs and M1 virus elicits a bystander killing effect, which is characterized by cell death in neighboring uninfected cells. To evaluate whether M1 virus induces some components synergized by SMCs to elicit the bystander killing effect, UV irradiation was used to inactivate M1 in the supernatant from M1-infected HCT 116 and Huh-7 cells (Fig. 2*C*). HCT 116 and Huh-7 cells treated with LCL161 plus UV-inactivated supernatant showed significantly decreased cell viability (Fig. 2 *D* and *E*). Moreover, denaturation of the proteins in the supernatant by boiling abrogated the effect (Fig. 2 *D* and *E*), indicating that the functional molecules in the UV-inactivated supernatants were proteins.

IL-8, IL-1A, and TRAIL Mediate the Bystander Killing Effect Potentiated by SMCs. As reported, a virus is a kind of immune stimulus with responses that include, in addition to antiviral IFNs, other growth-promoting or death-inducing cytokines (11). SMCs sensitize tumor cells to different cytokines, such as TNF-α, TRAIL, and IL-1β, and promote the bystander killing effect with these cytokines.

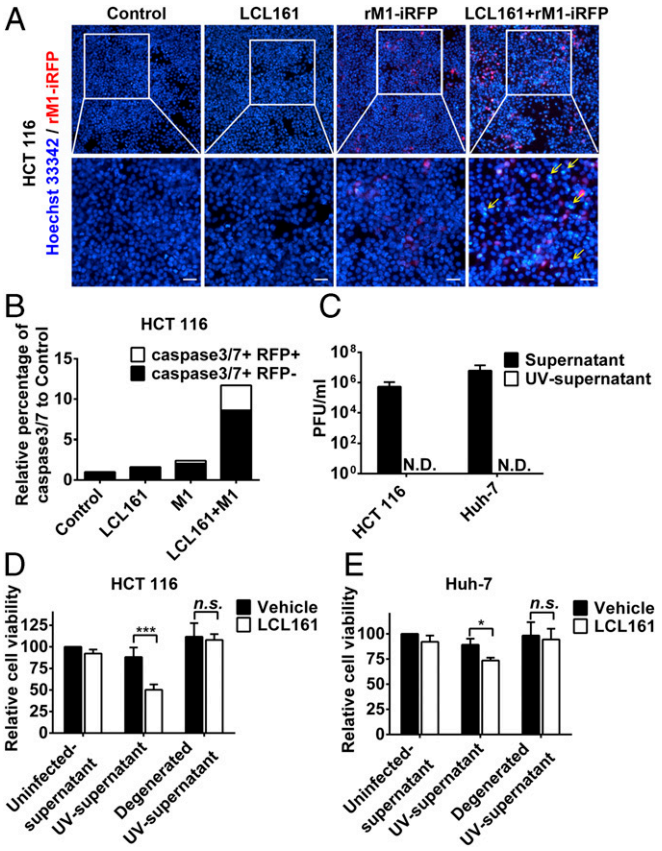

Fig. 2. SMCs synergize with M1 to potentiate the bystander killing effect. (*A*) HCT 116 cells were treated with recombinant M1 (rM1)-iRFP (MOI = 1 pfu/cell) with or without 5 μM LCL161 for 72 h and stained with Hoechst 33342. (Scale bars: 20 μm.) (*B*) Percentages of caspase-3/7$^{+/-}$ and iRFP$^{+/-}$ cells were detected using flow cytometry in HCT 116 cells treated as in *A*. (*C*) Effect of UV irradiation (1 h) on viability ($TCID_{50}$ method) of M1 in the supernatants. Supernatants were collected from HCT 116 and Huh-7 cells (MOI = 1 pfu/cell) infected with M1 for 48 h. (*D* and *E*) Ten percent of supernatants inactivated by UV irradiation in *C* were treated with or without boiling and were then combined with LCL161, after which cell viability was detected. Error bars represent mean ± SD obtained from three independent experiments. N.D., not detected; n.s., no significance; $TCID_{50}$, median tissue culture infectious dose. **P* < 0.05; ****P* < 0.001.

Therefore, proteins in the UV-supernatant synergized with SMCs are likely cytokines. To prove this hypothesis, we conducted an expression profile in HCT 116 cells treated with or without M1 and focused on the mRNA expression of 112 cytokines and chemokines in the array data based on related research on their induction of the bystander killing effect (14) and whole cellular cytokine and chemokine signaling pathways (14, 19). We ranked the cytokines and chemokines by the expression ratio upon M1 treatment compared with the control group (Fig. 3*A*). Among the 112 cytokines, we selected the top 10 [Fig. 3 *A* (red dots) and *B*], combined their recombinant proteins with LCL161, and analyzed their influence on the bystander killing effect. IL-1A, IL-8, and TRAIL synergized with LCL161 to induce cell death in HCT 116 and Huh-7 cells, but other cytokines did not (Fig. 3*C* and Fig. S3 *A*–*C*). The expression and secretion of IL-1A, IL-8, and TRAIL in mRNA and protein levels were also verified by RT-quantitative PCR and ELISA (Fig. 3 *D* and *E* and Fig. S3 *D* and *E*). On the other hand, the cytokines, such as TRAIL, did not increase M1 cytotoxicity in HCT 116 cells and just slightly increased cytotoxicity in Huh-7 cells, which was attributed to the addictive effect of TRAIL and M1 virus (Fig. S3*F*). In conclusion, IL-1A, IL-8, and TRAIL were induced by M1 virus to be potentiated by SMCs to elicit the bystander killing effect.

c-IAP1 and c-IAP2 Play Key Roles in the Enhanced Oncolytic Effect Induced by SMCs. The most studied and classical members of the IAP family, c-IAP1, c-IAP2, and XIAP, are often designated as targets of SMCs. In our model, only c-IAP1 and c-IAP2, but not XIAP, were inhibited by LCL161 and birinapant (Fig. 4 *A* and *B* and Fig. S4 *A* and *B*), indicating that they may play key roles in the enhanced oncolytic effect. To confirm this conclusion, we used siRNAs to knock down each of the proteins. Combination of sic-IAP1 or sic-IAP2 with M1, but not siXIAP, significantly reduced cell viability (Fig. 4 *C*–*H* and Fig. S4 *C*–*H*). These results indicate that only c-IAP1 and c-IAP2, but not XIAP, function to enhance the oncolytic effect of M1.

SMCs Increase the Replication of M1 and M1-Induced ER Stress-Mediated Apoptosis. We have previously shown that cancer-selective replication underlies the cancer targeting property of M1 (6, 15, 16). To understand whether the replication of M1 virus is affected by SMCs, we analyzed the effect of SMCs on the replication of M1 virus. The expression of viral proteins and RNA, as well as the titer of virus, increased on treatment with

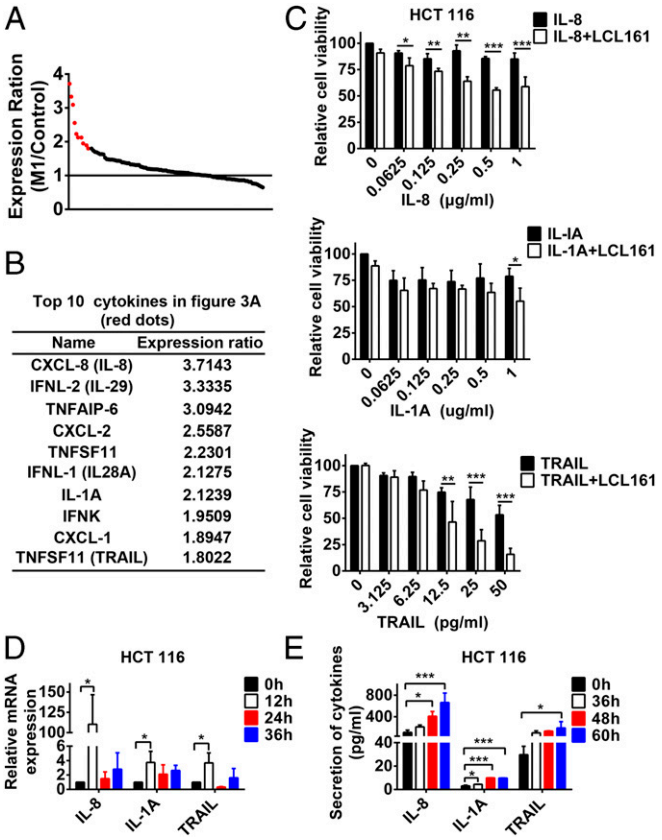

Fig. 3. IL-8, IL-1A, and TRAIL play key roles in the potentiated bystander killing effect. (*A*) Expression ratio of 112 cytokines relative to the control group was shown in HCT 116 cells infected with M1 (MOI = 1 pfu/cell) for 24 h. (*B*) Detailed information on the top 10 cytokines in *A* (red dots). (*C*) HCT 116 cells were treated with LCL161 or LCL161 plus different concentrations of recombinant proteins of IL-8, IL-1A, and TRAIL for 72 h, and cell viability was detected. HCT 116 cells were treated with M1 for different lengths of time, and mRNA level (*D*) and protein level (*E*) of IL-8, IL-1A, and TRAIL were detected with RT-quantitative PCR and ELISA. Error bars represent mean ± SD obtained from three independent experiments. **P* < 0.05; ***P* < 0.01; ****P* < 0.001.

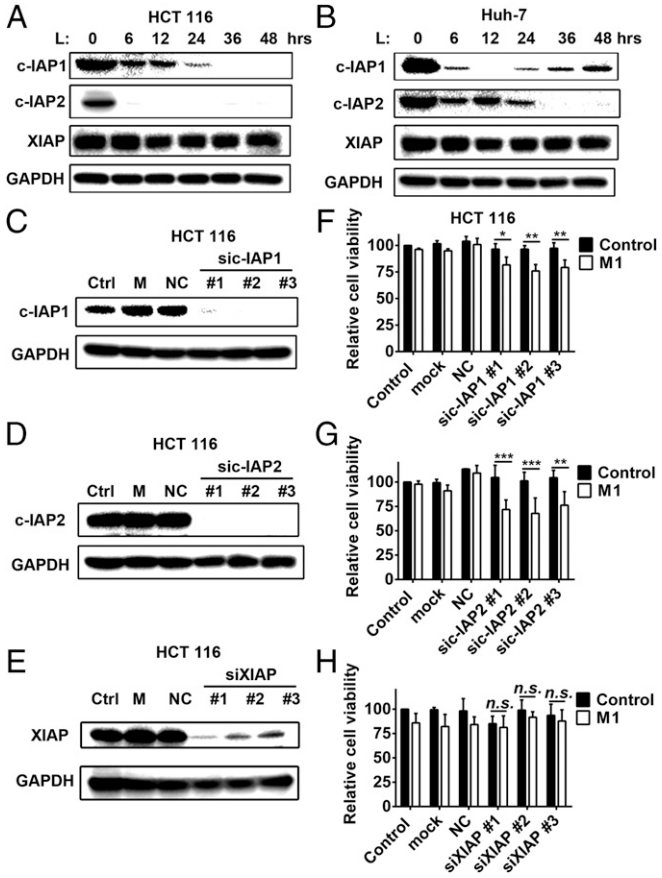

Fig. 4. c-IAP1 and c-IAP2 play key roles in the enhanced oncolytic effect induced by SMCs. The effect of LCL161 on expression of three classical IAPs in HCT 116 cells (*A*) and Huh-7 (*B*) cells is shown. The effect of siRNAs to c-IAP1 (*C*), c-IAP2 (*D*), and XIAP (*E*) on the protein level of each is shown. (*F–H*) HCT 116 cells were treated with siRNAs to cIAP1, cIAP2, and XIAP. Forty-eight hours later, M1 virus (MOI = 1 pfu/cell) was added for another 48 h and cell viability was detected. Error bars represent mean ± SD obtained from three independent experiments. L, LCL161; M, mock; NC, negative control. $*P < 0.05$; $**P < 0.01$; $***P < 0.001$.

LCL161 plus M1 (Fig. 5 *A–C* and Fig. S5 *A* and *B*). The knockdown of c-IAP1 and c-IAP2, but not XIAP, with specific siRNAs increased viral titer and proteins (Fig. 5*D* and Fig. S5 *C–I*). Additionally, the expression of viral proteins in the normal cell lines L-02 and NCM460 was undetectable under all of the treatments (Fig. S5*J*).

Increased replication induces the aggregation of viral protein in host cells, which, in turn, induces the unfolded protein response and changes in the ER (31), as observed using SEM (32). The combination of LCL161 and M1 induced severe ER swelling in HCT 116 and Huh-7 cells (Fig. S6 *A* and *B*), indicating irreversible ER stress. In three specific ER stress-mediated apoptosis pathways [CHOP, c-Jun N-terminal kinase (JNK) and caspase-12] (33), the expression of phosphorylated JNK was elevated on combined treatment, but CHOP and caspase-12 expression was not (Fig. S6 *C* and *D*). Taken together, these results suggest that SMCs increase the replication of M1 and that the accumulation of viral protein induces irreversible ER stress and cell apoptosis via the JNK, but not the caspase-12 or CHOP, pathway. Moreover, c-IAP1 and c-IAP2, but not XIAP, play key roles in this effect.

SMCs Synergize with M1 to Inhibit Tumor Progression in Vivo and ex Vivo. To investigate whether the effects of the combination of SMCs and M1 virus that we observed in vitro were also achievable in vivo, a xenograft tumor model was established in nude mice with HCT 116 and Huh-7 cells (Fig. 6*A* and Fig. S7*A*). The combination of LCL161 and M1 resulted in smaller tumors than in the other three experimental groups, therefore inhibiting tumor progression (Fig. 6 *B* and *C* and Fig. S7 *B* and *C*). Moreover, in each tumor, Ki67 was substantially downregulated and cleaved caspase-3 was correspondingly upregulated in the combined treatment group (Fig. 6 *D* and *E* and Fig. S7 *D* and *E*), indicating that the combination of LCL161 and M1 inhibits the malignant characteristics of the tumors in vivo. Further, in another HCT 116 tumor xenograft model using larger tumors over a prolonged period, which is more similar to the clinical situation, the combination of LCL161 and M1 virus still significantly inhibited tumor growth and delayed tumor progression (Fig. 6 *F* and *G*). Moreover, the replication of M1 virus is also increased in vivo (Fig. S7*F*). Consistent with the safety experiment in normal cell lines, none of the mice showed any abnormal pathology (Fig. S8). Finally, we examined the effect of the combination on primary human colon tumor surgical samples using tumor histoculture endpoint staining computer image analysis (34). Consistent with the in vivo results, the combination of LCL161 and M1 induced a greater percentage of death in four (patient 1 and patients 6–8) of the eight (50%) tumor tissues from patients with colon cancer (Fig. 6*H*). Moreover, the other four tumor tissues showing no combined effect were sensitive to LCL161, suggesting a therapeutic potential of the combined treatment strategy in LCL161-nonsensitive tumors.

Discussion

Our results identify SMCs as therapeutic agents to potentiate the oncolytic effect caused by M1 viral infection in vitro, in vivo, and ex vivo. SMCs or M1 alone induces only minimal tumor cell death, but their combination has a substantial killing effect. The mechanisms behind this effect have dual functions: (*i*) SMCs increase the replication of oncolytic virus M1 in HCT 116 colorectal tumor cells and Huh-7 hepatic tumor cells, achieving

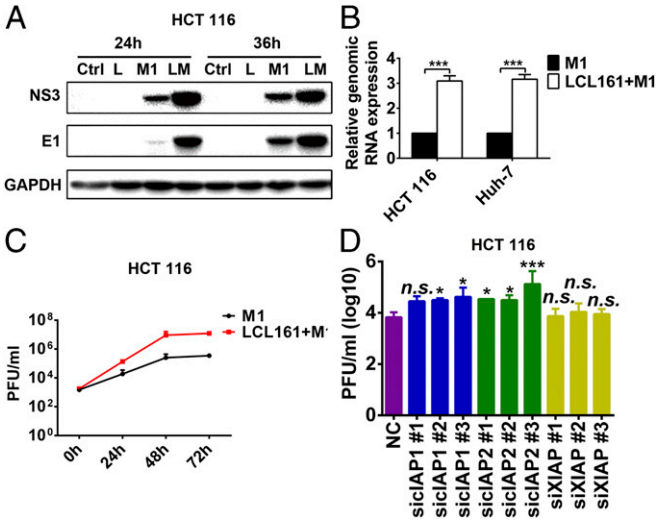

Fig. 5. LCL161 increases replication of M1 virus. The effect of LCL161 on replication of M1 at protein (MOI = 1 pfu/cell) (*A*), mRNA (MOI = 1 pfu/cell, 24 h postinfection) (*B*) and viral titer (*C*) levels in HCT 116 cells is shown. Viral titer (MOI = 0.1 pfu/cell) was detected with the $TCID_{50}$ method. (*D*) Effect of siRNAs to c-IAP1, c-IAP2, and XIAP on replication of M1 (MOI = 1 pfu/cell, 48 h postinfection) in HCT 116 cells. Viral titer was detected with the $TCID_{50}$ method. The viral yield of each treatment was compared with the NC group. Error bars represent mean ± SD obtained from three independent experiments. LM, LCL161 + M1. $*P < 0.05$; $***P < 0.001$.

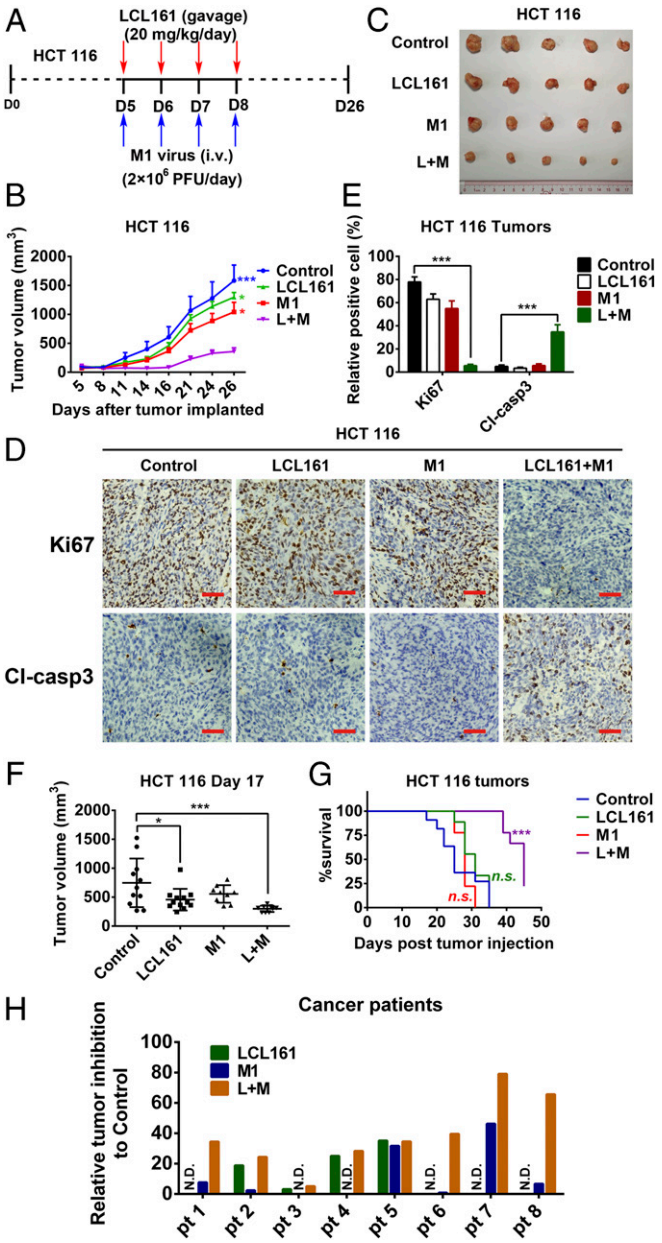

Fig. 6. Combination of LCL161 and M1 inhibits tumor progression in a mouse xenograft model and in human ex vivo tissues. (*A–C*) Effect of LCL161 and M1 combination on the mouse xenograft model with HCT 116 tumors ($n = 5$, tumor volume in each group was compared with the control group). D, day. (*D*) Intratumoral expression of Ki67 and cleaved caspase-3 (Cl-casp3) was detected by immunological histological chemistry in HCT 116 tumors. (Scale bars: 50 μm.) (*E*) Quantitation of cells positive for Ki67 and Cl-casp3 from multiple HCT 116 tumors and relative positive cells are shown ($n = 5$). (*F* and *G*) HCT 116 cells were implanted in nude mice when the tumor volume reached about 150 mm^3. Nude mice were treated with vehicle, LCL161, M1, and LCL161 plus M1 as in *A*. (*G*) According to the Animal Ethical and Welfare Committee of Sun Yat-sen University, when the tumor volume reached 1,500 mm^3, the mice were euthanatized for the survival curve drawing. (*F*) Tumor volume reached 1,500 mm^3 first in the control group at day 17 (control, $n = 12$; LCL161, $n = 12$; M1, $n = 9$; LCL161 + M1, $n = 9$.). (*H*) Surgical colon cancer specimens (50–100 mg) were cut into small pieces (~1 mm^3) and cultured in DMEM with 10% FBS and 5% penicillin/streptomycin at 37 °C. Tissues were then treated with vehicle (OPTI SFM), M1 (5×10^7 pfu), LCL161 (10 μM), and LCL161 (10 μM) plus M1 (5×10^7 pfu) for 3 d. Activity of tissues was measured by tissue culture end-point staining computer image analysis after staining with 3-(4,5-dimethylthiazol-2-yl)-2,5-diphenyltetrazolium bromide. The inhibition rates of each treatment for eight patients are shown. Error bars represent mean ± SD. pt, patient. $^*P < 0.05$; $^{***}P < 0.001$.

levels sufficient to cause tumor cell lysis, and (*ii*) SMCs sensitize these tumor cells to cytokines induced by M1, thus potentiating the bystander killing effect. Moreover, we identified the key cytokines in this potentiated bystander killing effect as IL-8, IL-1A, and TRAIL.

Although the intratumoral delivery of oncolytic viruses shows good outcomes in many clinical trials, systemic delivery will be required for metastatic cancers (2). However, the main limitation of systemic delivery is the intratumoral spread of oncolytic viruses, which are often attenuated by the host antiviral system. Although some cancer cells completely lack antiviral activity and can be successfully infected with oncolytic virus (35), most cancer cells are partially inactivated, which leads to limited sensitivity to the oncolytic virus (36). SMCs can increase the replication of M1 and the M1-induced bystander killing effect, thereby overcoming the limitation of systemic delivery in two ways. Moreover, some SMCs have already entered clinical trials, thus making the combined strategy more convenient in clinical application. In the future, we can arm M1 with Smac protein to enhance its replication and tumor-killing effect.

SMCs promote apoptosis by inhibiting functions of IAPs. In our model, SMCs also increase the replication of M1. The relationship between apoptosis and replication of oncolytic viruses is controversial. In the early stages of infection, viruses need tumor cells to be alive so they can take over and control the cellular molecular cell death machinery, but at later periods of infection, oncolytic viruses lyse and kill tumor cells to release newly assembled viruses (2). Some studies have reported that apoptosis limits the replication of influenza virus and other viruses (37–40), but others have found that promoting apoptosis activates the replication of human herpes virus and hepatitis B virus (41, 42). We found that neither pan-caspase inhibitors (Z-VAD-FMK and Q-VD-Oph) nor a JNK inhibitor (SP600125) abrogated the combined cytotoxicity (Fig. S9*A*), indicating that the virus replication mainly accounts for the combined cytotoxicity. Meanwhile, neither pan-caspase inhibitors nor the JNK inhibitor decreased the viral load (Fig. S9*B*), suggesting that the increased virus replication is independent of apoptosis. Our findings here provide an important building block to facilitate understanding of the relationship between apoptosis and viral replication, and may contribute to further investigations of the biological characteristics of viruses.

We report here another key mechanism by which SMCs synergize with M1 to kill tumor cells: the bystander killing effect. This mechanism is a newly identified method of tumor killing by the combination of vesicular stomatitis virus (VSV) and chemical agents (43). Combination of SMCs with M1 shows a tumor-killing mechanism (bystander killing) similar to the combination of SMCs and VSV, except that SMCs increase the replication of M1 but not VSV. By promoting M1 viral replication, the combination of SMCs and M1 presents advantages against tumors in two ways: (*i*) SMCs enhance the direct oncolysis as a result of increased M1 virus replication, and (*ii*) increasing M1 virus replication may stimulate more cytokines in tumor cells, which could be sensitized by SMCs to induce a stronger bystander killing effect. These findings provide a potential combined strategy to kill tumors.

A main concern in oncolytic virotherapy is the safety of the viruses; however, our results showed the combination of SMCs and M1 virus is exceptionally safe in animals. This finding suggests that the combined strategy is appropriate to treat cancers and is without side effects to normal organs.

In summary, our study shows that SMCs provide a significant benefit when combined with oncolytic virus M1. Our combined strategy overcomes the limitations of both SMCs and oncolytic virus M1 as single agents in tumor cells, murine models, and even in tumor tissues from patients, thus providing a promising strategy for treatment of human colorectal carcinoma and human hepatic carcinoma.

Materials and Methods

Cells, Reagents, and Virus. Cell lines were from the American Type Culture Collection and Shanghai Institute of Cell Biology, and were cultured in DMEM, Ham's F-12 nutrient medium, or RPMI-1640 supplied with 10% FBS and 1% penicillin/streptomycin (Life Technologies). All human primary cells were purchased from Sciencell Research Laboratories and cultured according to the instructions of the manufacturer. Specimens were obtained from consenting patients who underwent tumor resection. The institutional review board of Sun Yat-sen University Cancer Center has approved all human studies. All cells were cultured at 37 °C with 5% CO_2. LCL161 and birinapant were from Selleck, and were dissolved in DMSO at 10 mM. The caspase-3/7 flow cytometry assay kit was from Life Technologies (C10427). The strain of M1 virus has been described in our previous research (5, 6), and the virus was grown in the Vero cell line. The titer of virus was calculated by median tissue culture infectious dose assay in BHK-21 cell line.

Animal Models. The mouse study was approved by the Animal Ethical and Welfare Committee of Sun Yat-sen University.

Antibodies and Western Blot Assay. Cells were lysed by M-PER Mammalian Protein Extraction Reagent (Thermo Scientific), and the protein was resolved by SDS/PAGE. The primary antibodies are listed in *SI Materials and Methods*.

Caspase Activity Detection. Cells were cultured in 96-well plates in 100 μL of media and treated with different reagents (as listed in the figure legends). One hundred microliters of caspase-3/7, caspase-8, or caspase-9 (Promega) reaction buffer was added, and cells were cultured for another 30 min. Liquids were transferred to a black-bottomed, 96-well plate, and luminescence was detected using a Synergy H1 Microplate Reader (BioTek). The values were normalized to cell number [3-(4,5-dimethylthiazol-2-yl)-2,5-diphenyltetrazolium bromide assay].

Microarray Analysis. Total RNA was extracted from 1×10^6 cells with TRIzol Reagent (Life Technologies), and was sent to CapitalBio for labeling and hybridization to the Affymetrix GeneChip Human Genome U133 Plus 2.0 Array (Affymetrix). The data are accessible in the Gene Expression Omnibus (accession no. GSE92918). Functional analysis of differentially expressed genes was performed by DAVID (https://david.ncifcrf.gov/).

Statistical Analysis. All statistical analyses were performed using SPSS 19.0 software. Most of the data were analyzed by the Student *t* test or one-way ANOVA with Dunnett's tests for pairwise comparison. Tumor volumes were analyzed by repeated measures of ANOVA. Bars show the mean ± SD of at least three independent repeat experiments. The Wilcoxon signed rank test was used to compare paired nonnormally distributed data.

ACKNOWLEDGMENTS. We thank Prof. Liwu Fu and Caibo Yang for providing technical assistance in the ex vivo experiments, and Prof. Bernard Roizman, Prof. Guangping Gao, Prof. Shiyuan Chen, Prof. Wenbo Zhu, Prof. Jun Hu, Dr. Kai Li, Dr. Xiao Xiao, and Dr. Fan Xing for providing suggestions that improved this work. This work was funded by the National Natural Science Foundation of China (Grants 81573447 and 81603127); Natural Science Foundation of Guangdong Province, China (Grants 2016A030310160 and 2016A030310146); Science and Technology Planning Project of Guangdong Province, China (Grant 20160909); Research and Development Project of Applied Science and Technology of Guangdong Province, China (Grant 2016B020237004); and Science and Technology Planning Project of Guangdong Province, China (Grant 2015B020211003).

1. Parato KA, Senger D, Forsyth PA, Bell JC (2005) Recent progress in the battle between oncolytic viruses and tumours. *Nat Rev Cancer* 5:965–976.
2. Russell SJ, Peng KW, Bell JC (2012) Oncolytic virotherapy. *Nat Biotechnol* 30:658–670.
3. Andtbacka RH, et al. (2015) Talimogene laherparepvec improves durable response rate in patients with advanced melanoma. *J Clin Oncol* 33:2780–2788.
4. Pol J, Kroemer G, Galluzzi L (2015) First oncolytic virus approved for melanoma immunotherapy. *Oncoimmunology* 5:e1115641.
5. Hu J, Cai XF, Yan G (2009) Alphavirus M1 induces apoptosis of malignant glioma cells via downregulation and nucleolar translocation of p21WAF1/CIP1 protein. *Cell Cycle* 8:3328–3339.
6. Lin Y, et al. (2014) Identification and characterization of alphavirus M1 as a selective oncolytic virus targeting ZAP-defective human cancers. *Proc Natl Acad Sci USA* 111: E4504–E4512.
7. Zhang H, et al. (2016) Naturally existing oncolytic virus M1 is nonpathogenic for the nonhuman primates after multiple rounds of repeated intravenous injections. *Hum Gene Ther* 27:700–711.
8. Kaufman HL, Kohlhapp FJ, Zloza A (2015) Oncolytic viruses: A new class of immunotherapy drugs. *Nat Rev Drug Discov* 14:642–662.
9. Miest TS, Cattaneo R (2014) New viruses for cancer therapy: Meeting clinical needs. *Nat Rev Microbiol* 12:23–34.
10. Delwar Z, Zhang K, Rennie PS, Jia W (2016) Oncolytic virotherapy for urological cancers. *Nat Rev Urol* 13:334–352.
11. de Gruijl TD, Janssen AB, van Beusechem VW (2015) Arming oncolytic viruses to leverage antitumor immunity. *Expert Opin Biol Ther* 15:959–971.
12. Kirn DH, Thorne SH (2009) Targeted and armed oncolytic poxviruses: A novel multimechanistic therapeutic class for cancer. *Nat Rev Cancer* 9:64–71.
13. Cattaneo R, Miest T, Shashkova EV, Barry MA (2008) Reprogrammed viruses as cancer therapeutics: Targeted, armed and shielded. *Nat Rev Microbiol* 6:529–540.
14. Arulanandam R, et al. (2015) Microtubule disruption synergizes with oncolytic virotherapy by inhibiting interferon translation and potentiating bystander killing. *Nat Commun* 6:6410.
15. Li K, et al. (2016) Activation of cyclic adenosine monophosphate pathway increases the sensitivity of cancer cells to the oncolytic virus M1. *Mol Ther* 24:156–165.
16. Li K, et al. (2016) A classical PKA inhibitor increases the oncolytic effect of M1 virus via activation of exchange protein directly activated by cAMP 1. *Oncotarget* 7: 48443–48455.
17. McFadden G, Mohamed MR, Rahman MM, Bartee E (2009) Cytokine determinants of viral tropism. *Nat Rev Immunol* 9:645–655.
18. Kawai T, Akira S (2010) The role of pattern-recognition receptors in innate immunity: Update on toll-like receptors. *Nat Immunol* 11:373–384.
19. Alcami A (2003) Viral mimicry of cytokines, chemokines and their receptors. *Nat Rev Immunol* 3:36–50.
20. Fulda S, Vucic D (2012) Targeting IAP proteins for therapeutic intervention in cancer. *Nat Rev Drug Discov* 11:109–124.
21. Chai J, et al. (2000) Structural and biochemical basis of apoptotic activation by Smac/DIABLO. *Nature* 406:855–862.
22. Li L, et al. (2004) A small molecule Smac mimic potentiates TRAIL- and TNFalpha-mediated cell death. *Science* 305:1471–1474.
23. Petersen SL, et al. (2007) Autocrine TNFalpha signaling renders human cancer cells susceptible to Smac-mimetic-induced apoptosis. *Cancer Cell* 12:445–456.
24. Lalaoui N, et al. (2016) Targeting p38 or MK2 enhances the anti-leukemic activity of Smac-mimetics. *Cancer Cell* 29:145–158.
25. Fulda S, Wick W, Weller M, Debatin KM (2002) Smac agonists sensitize for Apo2L/TRAIL- or anticancer drug-induced apoptosis and induce regression of malignant glioma in vivo. *Nat Med* 8:808–815.
26. Deng Y, Lin Y, Wu X (2002) TRAIL-induced apoptosis requires Bax-dependent mitochondrial release of Smac/DIABLO. *Genes Dev* 16:33–45.
27. Cheung HH, et al. (2010) Smac mimetic compounds potentiate interleukin-1beta-mediated cell death. *J Biol Chem* 285:40612–40623.
28. Weisberg E, et al. (2010) Smac mimetics: Implications for enhancement of targeted therapies in leukemia. *Leukemia* 24:2100–2109.
29. Krepler C, et al. (2013) The novel SMAC mimetic birinapant exhibits potent activity against human melanoma cells. *Clin Cancer Res* 19:1784–1794.
30. Chou TC, Motzer RJ, Tong Y, Bosl GJ (1994) Computerized quantitation of synergism and antagonism of taxol, topotecan, and cisplatin against human teratocarcinoma cell growth: A rational approach to clinical protocol design. *J Natl Cancer Inst* 86: 1517–1524.
31. Walter P, Ron D (2011) The unfolded protein response: From stress pathway to homeostatic regulation. *Science* 334:1081–1086.
32. Wu J, Kaufman RJ (2006) From acute ER stress to physiological roles of the unfolded protein response. *Cell Death Differ* 13:374–384.
33. Szegezdi E, Logue SE, Gorman AM, Samali A (2006) Mediators of endoplasmic reticulum stress-induced apoptosis. *EMBO Rep* 7:880–885.
34. Furukawa T, Kubota T, Hoffman RM (1995) Clinical applications of the histoculture drug response assay. *Clin Cancer Res* 1:305–311.
35. Stojdl DF, et al. (2000) Exploiting tumor-specific defects in the interferon pathway with a previously unknown oncolytic virus. *Nat Med* 6:821–825.
36. Haralambieva I, et al. (2007) Engineering oncolytic measles virus to circumvent the intracellular innate immune response. *Mol Ther* 15:588–597.
37. Chang P, et al. (2015) Early apoptosis of porcine alveolar macrophages limits avian influenza virus replication and pro-inflammatory dysregulation. *Sci Rep* 5:17999.
38. Weiss R, et al. (2015) Interleukin-24 inhibits influenza A virus replication in vitro through induction of toll-like receptor 3 dependent apoptosis. *Antiviral Res* 123:93–104.
39. Kim SJ, et al. (2014) Hepatitis C virus triggers mitochondrial fission and attenuates apoptosis to promote viral persistence. *Proc Natl Acad Sci USA* 111:6413–6418.
40. Meng G, et al. (2014) Mitophagy promotes replication of oncolytic Newcastle disease virus by blocking intrinsic apoptosis in lung cancer cells. *Oncotarget* 5:6365–6374.
41. Wang YC, Yang X, Xing LH, Kong WZ (2013) Effects of SAHA on proliferation and apoptosis of hepatocellular carcinoma cells and hepatitis B virus replication. *World J Gastroenterol* 19:5159–5164.
42. Prasad A, Remick J, Zeichner SL (2013) Activation of human herpesvirus replication by apoptosis. *J Virol* 87:10641–10650.
43. Beug ST, et al. (2014) Smac mimetics and innate immune stimuli synergize to promote tumor death. *Nat Biotechnol* 32:182–190.
44. Lee SY, et al. (2006) Preliminary study of chemosensitivity tests in osteosarcoma using a histoculture drug response assay. *Anticancer Res* 26:2929–2932.